X-ray coherent scattering form factors of tissues, water and plastics using energy dispersion

2011 Phys. Med. Biol. 56 4377

(http://iopscience.iop.org/0031-9155/56/14/010)

Phys. Med. Biol. 56 (2011) 4377–4397 doi:10.1088/0031-9155/56/14/010

X-ray coherent scattering form factors of tissues, water and plastics using energy dispersion

B W King[1], **K A Landheer**[1] **and P C Johns**[1,2]

[1] Ottawa Medical Physics Institute, Department of Physics, Carleton University, 1125 Colonel By Drive, Ottawa, Ontario K1S 5B6, Canada
[2] Department of Radiology, University of Ottawa, Canada

E-mail: brian.king@newcastle.edu.au

Received 18 October 2010, in final form 18 April 2011
Published 27 June 2011
Online at stacks.iop.org/PMB/56/4377

Abstract

A key requirement for the development of the field of medical x-ray scatter imaging is accurate characterization of the differential scattering cross sections of tissues and phantom materials. The coherent x-ray scattering form factors of five tissues (fat, muscle, liver, kidney, and bone) obtained from butcher shops, four plastics (polyethylene, polystyrene, lexan (polycarbonate), nylon), and water have been measured using an energy-dispersive technique. The energy-dispersive technique has several improvements over traditional diffractometer measurements. Most notably, the form factor is measured on an absolute scale with no need for scaling factors. Form factors are reported in terms of the quantity $x = \lambda^{-1}\sin(\theta/2)$ over the range 0.363–9.25 nm^{-1}. The coherent form factors of muscle, liver, and kidney resemble those of water, while fat has a narrower peak at lower x, and bone is more structured. The linear attenuation coefficients of the ten materials have also been measured over the range 30–110 keV and parameterized using the dual-material approach with the basis functions being the linear attenuation coefficients of polymethylmethacrylate and aluminum.

1. Introduction

A library of the scattering properties of tissues and phantom materials will be an important tool for the developing field of x-ray scatter imaging (Leclair and Johns 2001). The differential scattering cross section per electron, $\mathrm{d}_e\sigma/\mathrm{d}\Omega$, determines the probability of photons with energy E scattering through an angle θ. The cross section is determined by a material's coherent (F_{coh}) and incoherent (F_{inc}) scattering form factors (Johns and Cunningham 1983):

$$\frac{\mathrm{d}_e\sigma}{\mathrm{d}\Omega} = \frac{\mathrm{d}_e\sigma_0}{\mathrm{d}\Omega}\left[F_{coh}^2(x) + F_{KN}(E,\theta)F_{inc}(x)\right]. \quad (1)$$

In this equation, $d_e\sigma_0/d\Omega$ is the classical Thomson cross section for scattering from a single, free electron and F_{KN} is the Klein–Nishina factor for incoherent scattering. Both form factors are functions of the momentum transfer argument:

$$x = \frac{1}{\lambda}\sin\left(\frac{\theta}{2}\right) = \frac{E}{hc}\sin\left(\frac{\theta}{2}\right), \tag{2}$$

where h is Planck's constant and c is the speed of light. For a given material, incoherent scattering can be accurately characterized for all values of x by computing F_{inc} as a combination of individual free atom form factors, such as those tabulated in Hubbell and Øverbø (1979). This is the independent atom model (IAM) approach. In the case of coherent scattering, however, interference effects dominate for small x, meaning that F_{coh} must be measured experimentally. Taking the practical limits of scatter imaging in diagnostic radiology in terms of angle and photon energy as $0.5° \leqslant \theta \leqslant 179°$, $16 \leqslant E \leqslant 140$ keV, a library of form factors for tissues and phantom materials is required from $x \sim 0.1$ nm^{-1} through to the IAM region, $x \sim 10$ nm^{-1}.

For pure water, the gold standard for F_{coh} is the dataset of Narten (1970) who published data for $0 \leqslant x \leqslant 12.7$ nm^{-1}. For tissues, the seminal paper was that of Kosanetzky *et al* (1987), who published angle-dispersive diffractometer curves for $0.25 \leqslant x \leqslant 4.3$ nm^{-1} for pork fat, muscle, tendon, bone, blood, liver, brain white matter, and brain grey matter, and the synchrotron work of Peplow and Verghese (1998) who studied several normal animal tissue types out to $x = 10$ nm^{-1} with the minimum x between 0.42 and 1.08 nm^{-1}, sample dependent. Others looked at a restricted range of materials and/or of x values (Evans *et al* 1991, Royle and Speller 1995, Westmore *et al* 1996, Tartari *et al* 1997, Kidane *et al* 1999, Lewis *et al* 2000, Desouky *et al* 2001, Poletti *et al* 2002, Fernández *et al* 2002, Castro *et al* 2004, Griffiths *et al* 2007, Elshemey *et al* 2010). Most of these measurements used angle-dispersive diffractometers, which were either conventional crystallographic machines or synchrotron instruments. Angle-dispersive diffractometers have inherent problems in measuring F_{coh} for amorphous materials such as tissues and the published results vary significantly (Johns and Wismayer 2004). We have reported on alternative methods of measuring form factors that can be done simply using a photostimulable phosphor plate but are low in x-resolution (King and Johns 2008).

Most recently, we have thoroughly characterized an energy-dispersive method that provides reliable measurements for tissue-like materials (King and Johns 2010). In this approach, a polychromatic x-ray tube source and energy-dispersive detector are aligned and the specimen is moved laterally so that photons must scatter at a small θ to reach the detector. This configuration is based on earlier work in our lab (Leclair and Johns 2002, Hasan 2003, Hasan and Johns 2004, King 2009) and a similar approach was taken by Kidane *et al* (1999) and Leclair *et al* (2006). Here we report coherent scatter form factors of tissues, water, and plastics based on this energy-dispersive technique.

2. Theory

The basic geometry of the experiment is shown in figure 1. More detailed information on the experimental configuration and the derivation of the following equations can be found in our previous work (King and Johns 2010). An x-ray tube acts as a polychromatic source of x rays and the detector is an x-ray spectrometer. By translating the target laterally, the number of photons can be measured in both a transmission and a scatter configuration. The x-ray source and spectrometer remain stationary throughout the experiment.

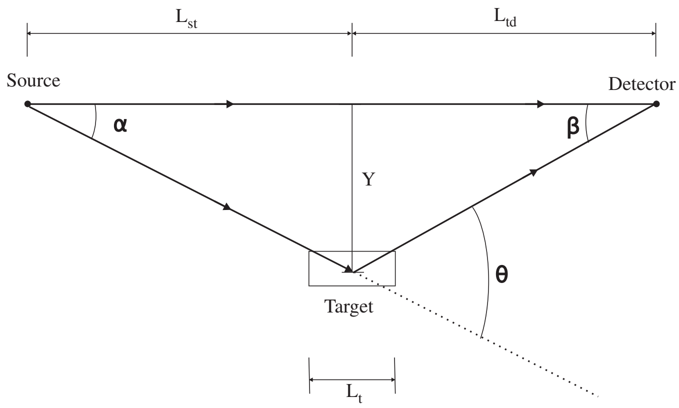

Figure 1. Schematic geometry of the energy-dispersive experiment.

In the transmission configuration, we have shown previously (King and Johns 2010) that if the differential fluence per energy interval from the x-ray source at a distance L_{st} is $\mathrm{d}\Phi_{t0}/\mathrm{d}E$, the number of photons in the range $E \rightarrow E+\mathrm{d}E$ measured by the detector with cross-sectional area A_{dt} through a target with linear attenuation coefficient $\mu_t(E)$ will be

$$\mathrm{d}N_t(E) = \mathrm{d}\Phi_{t0}\frac{L_{st}^2}{(L_{st}+L_{td})^2}A_{dt}\exp[-\mu_t(E)L_t]\,. \tag{3}$$

In the scattering configuration, if the x-ray source differential fluence at a distance L_{st} is $\mathrm{d}\Phi_{s0}/\mathrm{d}E$, the number of photons measured is

$$\mathrm{d}N_s(E) = \frac{\mathrm{d}\Phi_{s0}(E)L_{st}^2\rho_e V_t A_{ds}\cos\beta}{\left(L_{st}^2+Y^2\right)\left(L_{td}^2+Y^2\right)}\exp[-\mu_t(E)L_t]\frac{\mathrm{d}_e\sigma}{\mathrm{d}\Omega} \tag{4}$$

where A_{ds} is the area of the detector, ρ_e is the electron density of the target material and V_t is the scattering volume of the target. This expression is only valid for $\cos\alpha \approx \cos\beta \approx 1$. In our experiment, α is at most 7.94° and β is at most 7.15° (King and Johns 2010). Then, by computing the ratio of the scatter and transmitted spectra and using the definition of $\mathrm{d}_e\sigma/\mathrm{d}\Omega$ from equation (1), an expression for the coherent scattering form factor can be found:

$$F_{coh}(x) = \left\{\left[\frac{\left(L_{st}^2+Y^2\right)\left(L_{td}^2+Y^2\right)}{(L_{st}+L_{td})^2\frac{\mathrm{d}_e\sigma_0}{\mathrm{d}\Omega}\rho_e V_t\cos\beta}\right]\left[\frac{A_{dt}}{A_{ds}}\frac{\mathrm{d}\Phi_{t0}}{\mathrm{d}\Phi_{s0}}\frac{\mathrm{d}N_s(E)}{\mathrm{d}N_t(E)}\right] - F_{KN}(E,\theta)F_{inc}(x)\right\}^{1/2}. \tag{5}$$

In order to compute F_{coh} from this expression, the composition of the target material must be known so that ρ_e and F_{inc} can be generated from tables.

Although measurement of F_{coh} is the main goal of this work, the data provide additional useful information. The differential linear scattering coefficient (Kosanetzky *et al* 1987, Leclair *et al* 2006) is analogous to the linear attenuation coefficient μ_t but is the probability per unit distance travelled of scattering into a given solid angle:

$$\mu_s = \rho_e \mathrm{d}_e\sigma/\mathrm{d}\Omega\,. \tag{6}$$

Both coherent and incoherent scattering information for the material are contained in this definition. From equations (3) and (4),

$$\mu_s(E,\theta) = \left[\frac{\left(L_{st}^2+Y^2\right)\left(L_{td}^2+Y^2\right)}{(L_{st}+L_{td})^2 V_t\cos\beta}\right]\left[\frac{A_{dt}}{A_{ds}}\right]\left[\frac{\mathrm{d}\Phi_{t0}}{\mathrm{d}\Phi_{s0}}\right]\left[\frac{\mathrm{d}N_s(E)}{\mathrm{d}N_t(E)}\right]. \tag{7}$$

The advantage of measuring μ_s is that the composition of the material does not need to be known. Thus, μ_s can be extracted more easily from scatter measurements. The quantity μ_s is not simply a function of the single variable x, however, but varies with both E and θ due to the presence of the Klein–Nishina factor F_{KN} in the scattering cross section. For low energies, F_{KN} approaches 1 so this difference is small but at higher energies it is more important.

In order to remove the effect of any background photons (i.e. photons scattered in the container walls or elsewhere), for both the scatter and the transmission configurations we measured spectra with none of the target material present.

From our data, it was straightforward to also determine the linear attenuation coefficient of the material μ_t as a function of energy, using the two transmission measurements, i.e. with and without the target material. In the absence of K-edges, the attenuation coefficient can be parameterized in a dual-material decomposition (Lehmann *et al* 1981) using two basis materials α and β:

$$\mu_t(E) = a_\alpha \mu_\alpha(E) + a_\beta \mu_\beta(E) \tag{8}$$

where μ_α and μ_β are the linear attenuation coefficients of the basis materials and a_α, a_β are fitting parameters determined from the measured data. The parameters can also be expressed in polar coordinates r and Φ.

3. Experimental details

3.1. Apparatus

Our experimental setup was described in detail previously and fully characterized (King and Johns 2010). Here, we summarize some of the important points. We used a Machlett-Dynamax rotating anode tungsten x-ray tube as a source of polychromatic x rays. A potential of 121 kV was used with a nominal current of 2 mA. A PTW (PTW, Freiburg, Germany) Farmer style ion chamber was used to measure the beam output. All measurements were normalized to the output of this chamber. Apertures before and after the target defined seven different θ as well as the transmission configuration. Values for θ ranged from 1.7° to 15.1° (see table 1). An Ortec HPGe spectrometer (Ortec, Oak Ridge, TN, USA) was used to measure all spectra. The x-ray tube and spectrometer were aligned for the transmission configuration and were then fixed in place. A very small aperture was constructed for the transmission configuration by mounting a pair of micrometer spindles with tungsten carbide tips behind a 0.5 mm pinhole in a Pb sheet to give an aperture of roughly 20 μm $\times$ 500 μm. This aperture was removed during the measurement of the scatter spectra. The target was translated laterally to align in turn with each scatter aperture. In each configuration, both transmission and scatter spectra were measured with the target present in the path of the beam and without the target material. For liquid or tissue materials, this background was measured with an empty target container. For solid materials, the background was measured with nothing in the path of the beam. The scattering volume was calculated using a Monte Carlo ray-tracing simulation of the experiment developed in Matlab (The Mathworks, Natick, MA, USA).

The individual results from each configuration were combined together on a common grid in x space. Where different configurations overlapped, the results were checked for consistency with a χ^2 test. If the data were consistent, a weighted average was computed. Otherwise, for isolated inconsistencies, an unweighted average was used, and for regions with multiple inconsistencies the highest x resolution value was used. The rationale for this procedure is that a string of inconsistent values most likely corresponds to a sharp peak in the form factor where the varying resolutions from different configurations blur the peak to different extents.

Table 1. Details of the seven different scatter configurations used in the experiment. The range of x accessible is based on a usable spectrum between 30 and 110 keV. The uncertainty in x given here is the mean uncertainty over all energies.

Configuration	Scattering angle (degrees)	x accessible (nm^{-1})	x uncertainty (%)
Scatter 1	1.67 ± 0.17	0.35–1.29	5.5
Scatter 2	3.17 ± 0.15	0.67–2.45	3.3
Scatter 3	5.03 ± 0.15	1.06–3.89	2.6
Scatter 4	6.30 ± 0.15	1.33–4.87	2.4
Scatter 5	10.05 ± 0.17	2.12–7.77	2.3
Scatter 6	12.58 ± 0.17	2.65–9.72	2.2
Scatter 7	15.09 ± 0.17	3.18–11.65	2.2

Table 2. Material parameters, compositions and number of repeated measurements for the materials studied. The density of water is given at 22.5 °C. The number of repeated measurements for each material is given as N.

Material	Composition	ρ (g cm^{-3})	ρ_e (cm^{-3})	N
Water	H_2O	0.9982	3.3348×10^{23}	5
Polyethylene	$(C_2H_4)_n$	0.948	3.255×10^{23}	5
Polystyrene	$(C_8H_8)_n$	1.042	3.373×10^{23}	1
Polycarbonate	$(C_{16}H_{14}O_3)_n$	1.17	3.71×10^{23}	1
Nylon	$(C_6H_{11}NO)_n$	1.138	3.753×10^{23}	1
Fat	From ICRP 23 (1975)	0.92	3.09×10^{23}	2
Muscle	From ICRP 23 (1975)	1.04	3.44×10^{23}	3
Liver	From Kosanetzky *et al* (1987)	1.045	3.48×10^{23}	3
Kidney	From ICRP 23 (1975)	1.05	3.48×10^{23}	1
Bone	From Woodard (1962)	1.85	5.73×10^{23}	1

3.2. Sample preparation

The tissues studied were fat, muscle, liver, kidney and bone. Water and four plastics were also studied. The composition and physical parameters of these materials can be found in table 2.

All samples were butcher-shop beef except for the fat samples which were pork, and were refrigerated, but not frozen, before use. All tissue samples except for the bone were placed in a 4 cm long custom built polycarbonate container. The entrance and exit windows were each 0.5 mm thick. The length of the container was designed to provide the largest scattering volume and hence, scattering signal possible. The tissue samples were cut to fit the container as tightly as possible. To prevent dehydration, the container was filled with phosphate-buffered saline and then the tissue was inserted, displacing the solution without air entrapment. Wherever possible, single pieces of tissue were used to fill the container.

The bone sample was placed in a shorter container (0.66 cm long) because of the larger amount of attenuation and multiple scattering present in this sample. The entrance and exit windows were again 0.5 mm thick. The shorter container, however, gave a reduced signal for the smaller scattering angles and increased the uncertainty of the volume calculation.

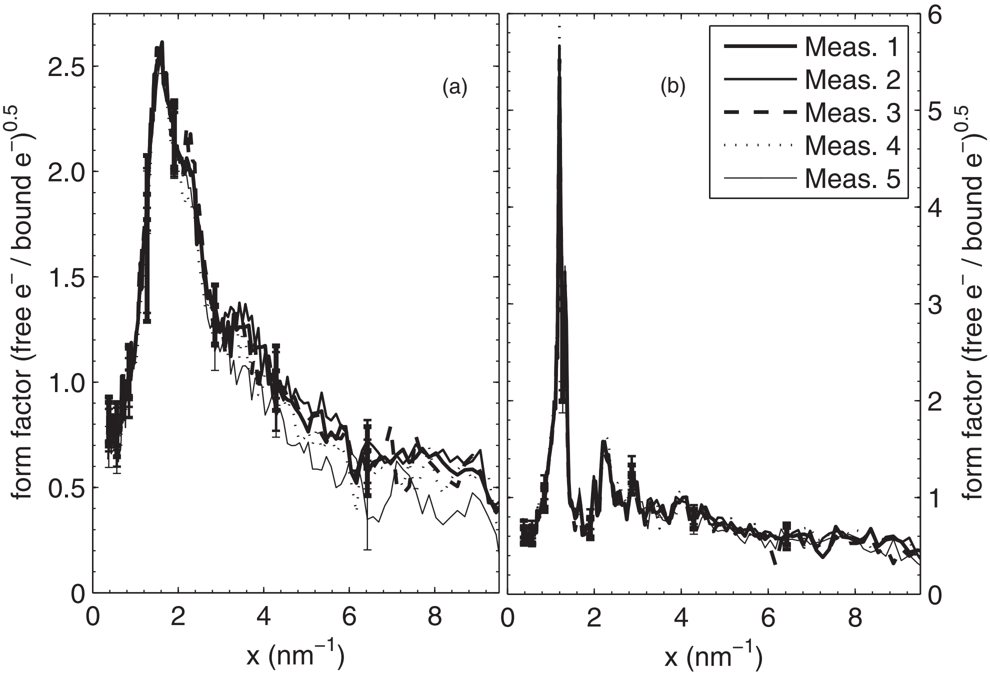

Figure 2. Results of repeated form factor measurements of (a) water and (b) polyethylene. Error bars are shown only for every 20th point for clarity.

4. Results

Water and polyethylene were used as control samples with measurements being repeated five times over a period of roughly six weeks to ensure the reliability of the measurements. The results are shown in figure 2.

The other plastic materials were each measured a single time. Measured form factors for polystyrene, polycarbonate (lexan) and nylon are shown in figure 3. Tissue measurements were repeated multiple times, using different samples, to assess how much variation in the form factors can be expected. The results can be found in figures 4 and 5. Where measurements were repeated, the mean value was used and the uncertainties shown in the graphs represent the standard deviation of the results. All of the measured values of F_{coh}, μ_{s} and μ_{t} and their uncertainties are tabulated in the appendix.

The measured attenuation coefficient of water (table A1) was compared to two standard references. When compared to Plechaty *et al* (1975), μ_{t} was larger by 3.3% at 40 keV, 5.6% at 60 keV, 5.2% at 80 keV and 2.9% at 100 keV. In comparison to the more recent NIST XCOM database (Berger *et al* 2010), the differences were 1.2% at 40 keV, 4.9% at 60 keV, 4.9% at 80 keV and 2.8% at 100 keV. These differences are within our measurement uncertainty at 100 keV and somewhat outside at lower energies depending on which dataset is used for comparison.

The dual-material decompositions of $\mu_{\mathrm{t}}(E)$, as outlined in section 2, are shown in table 3. The dual-material fitting parameters were computed by performing a χ^2 minimization of the measured attenuation coefficients to those predicted by equation (8) for energies between 30 and 110 keV. The basis materials used were Al and polymethylmethacrylate (PMMA). The attenuation coefficients of the basis materials were taken from Plechaty *et al* (1975).

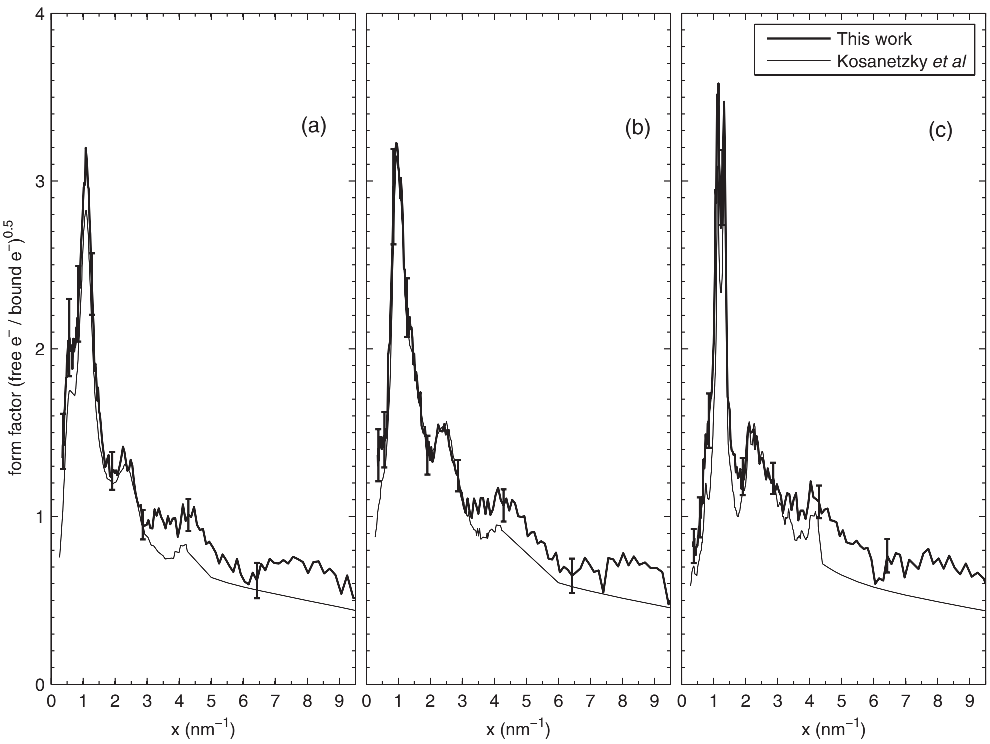

Figure 3. Measured form factors of (a) polystyrene, (b) polycarbonate, and (c) nylon as compared to diffractometer-based measurements by Kosanetzky *et al* (1987). Error bars are shown only for every 20th point for clarity. Data were taken from the paper of Kosanetzky *et al* to 4.3 nm^{-1}. At high x we used Independent Atom Model results, and at intermediate x a smooth transition between the two.

Table 3. Dual-material decompositions of μ_t for the ten materials studied. Values of r and Φ give the polar coordinates of the decomposition, where Φ is the angle from the a_{PMMA} axis. There were 155 degrees of freedom for each set of fitting parameters.

Material	a_{PMMA}	a_{Al}	r	Φ (degrees)	χ^2
Water	0.879 ± 0.013	0.0197 ± 0.0012	0.880 ± 0.012	1.28 ± 0.08	168
Polyethylene	0.910 ± 0.012	-0.0200 ± 0.0010	0.910 ± 0.012	-1.26 ± 0.06	148
Polystyrene	0.952 ± 0.015	-0.0198 ± 0.0018	0.952 ± 0.015	-1.19 ± 0.10	129
Polycarbonate	1.005 ± 0.015	-0.0054 ± 0.0015	1.005 ± 0.015	-0.31 ± 0.09	130
Nylon	1.036 ± 0.015	-0.0110 ± 0.0015	1.036 ± 0.015	-0.61 ± 0.08	125
Fat	0.823 ± 0.011	-0.0028 ± 0.0010	0.823 ± 0.011	-0.20 ± 0.07	131
Muscle	1.059 ± 0.015	0.0113 ± 0.0011	1.059 ± 0.015	0.61 ± 0.06	231
Liver	0.952 ± 0.014	0.0265 ± 0.0010	0.952 ± 0.014	1.59 ± 0.07	184
Kidney	0.860 ± 0.014	0.0309 ± 0.0019	0.861 ± 0.014	2.06 ± 0.14	136
Bone	-0.23 ± 0.04	0.84 ± 0.03	0.87 ± 0.03	105.2 ± 2.6	115

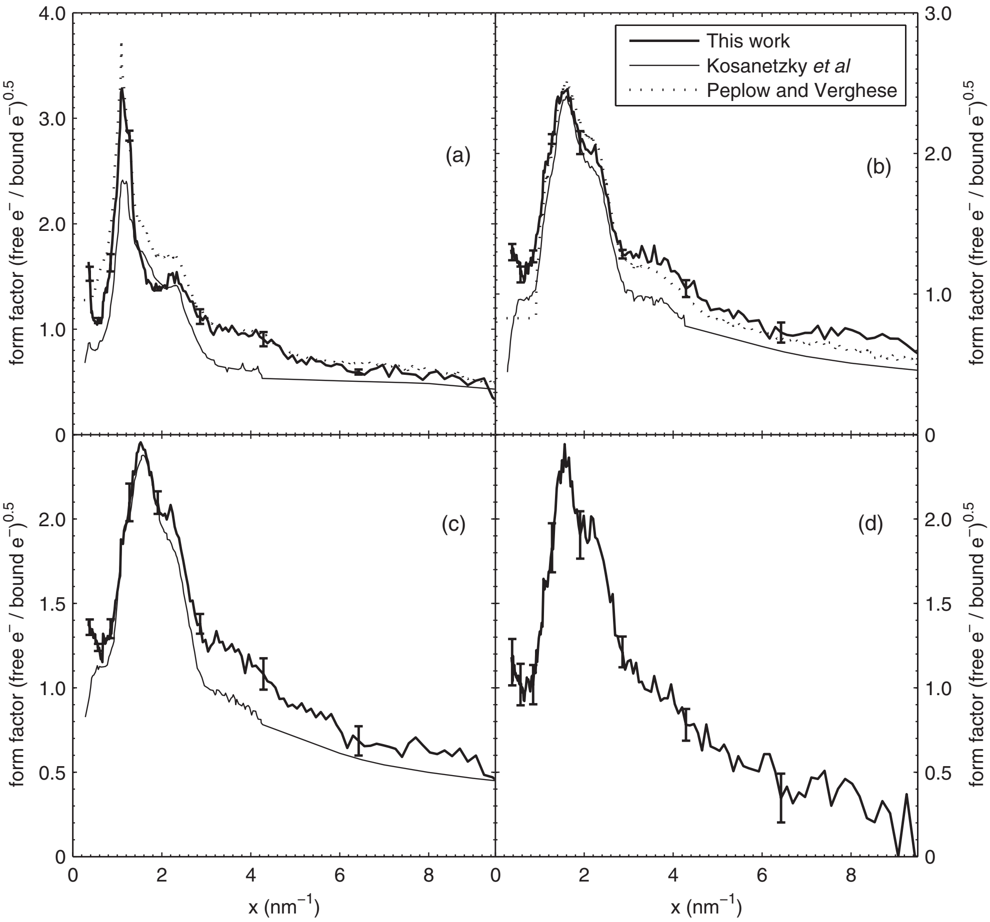

Figure 4. Measured form factors of (a) fat, (b) muscle, (c) liver and (d) kidney. Error bars are shown only for every 20th point for clarity. The results are compared to measurements from the literature where available (Kosanetzky *et al* 1987, Peplow and Verghese 1998). Data were taken from the paper of Kosanetzky *et al* to 4.3 nm^{-1}. At high x we used Independent Atom Model results, and at intermediate x a smooth transition between the two.

5. Discussion and conclusion

The measured form factors of the tissues are very similar to water, with the exception of the fat sample. This is consistent with the fact that the soft tissues are composed primarily of water. The tissues all show a strong increase in the form factor for $x \lesssim 0.5$ nm^{-1} that was not visible in diffractometer results. As this increase is not present in the water and plastic measurements, we conclude that this is a real feature of the tissue scattering. This may be a result of longer range structure present in tissues as compared to water. However, the results for small x values are quite uncertain and should be verified through measurements at lower energies.

The size of the sample is an important factor in the design of the experiment. A larger scattering volume will produce more scattered photons and hence a stronger signal. A larger sample also leads to smaller geometric uncertainties. As the geometric uncertainties constitute the dominant source of uncertainties in the results, this is an important factor. The effect of

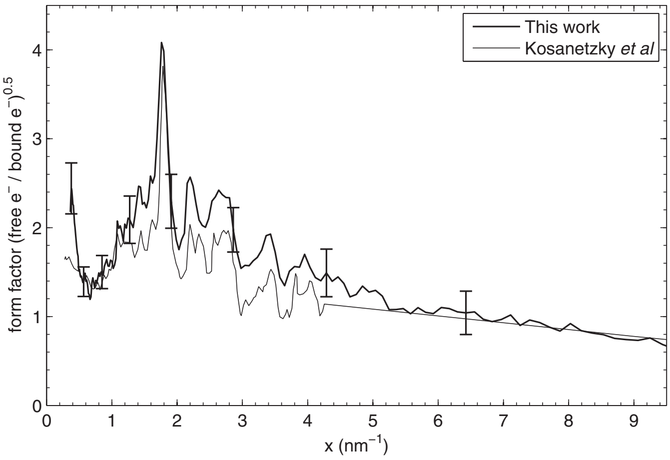

Figure 5. Measured form factor of bone. The results are compared to diffractometer measurements from the literature (Kosanetzky *et al* 1987). Error bars are shown only for every 20th point for clarity. Data were taken from the paper of Kosanetzky *et al* to 4.3 nm^{-1} while at high x we used Independent Atom Model results.

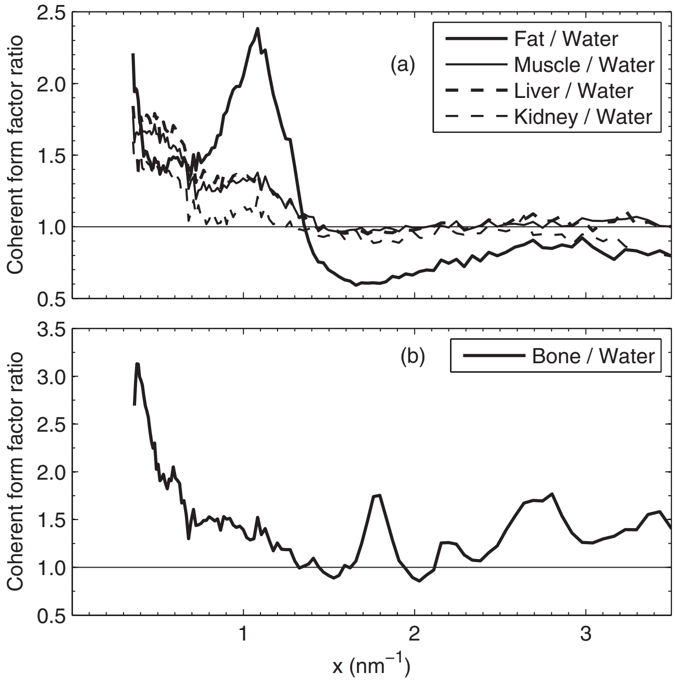

Figure 6. Ratio of (a) soft tissue and (b) bone coherent scattering form factors compared to water for $0.363 \leqslant x \leqslant 3.5$ nm^{-1}.

the smaller sample size can be seen by comparing the uncertainties of the tissue measurements to those of the bone sample. However, a larger sample also makes it more difficult to prepare pure samples for measurement. Some types of tissues were unable to be studied because pure samples of the required size could not be obtained. As an example, in our work, grey and white brain tissue have not yet been separated clearly enough from each other to be distinguished.

The measured values of F_{coh} at large x values are quite noisy. This is a result of the limited number of coherently scattered photons in these regions. Extracting the small coherently scattered signal from the much larger incoherent contribution is quite difficult. On the other hand, since the coherently scattered photons represent such a small fraction of those scattered in this region, an accurate knowledge of F_{coh} is less critical than for smaller values of x where coherent scattering is the dominant mechanism.

The feasibility of using coherent scattering to distinguish between different types of materials was investigated by computing the ratio of the tissue form factors to that of water in figure 6. Fat shows the strongest difference from water, owing to the structural differences present between the two. The other soft tissues studied are much more similar. All of the soft tissues exhibit a peak around 1 nm^{-1} which we ascribe to the fat content. In this region, it appears that imaging will yield the most contrast. Further study of these and other tissues may identify other cases where coherently scattered photons can play a diagnostic role.

Acknowledgments

This work was supported by the Natural Sciences and Engineering Research Council of Canada. Thanks are extended to Philippe Gravelle in the Carleton University Physics Department machine shop for general fabrication assistance and Dr David Rogers for loan of a dual channel electrometer.

Appendix A. Measured data

Table A1 gives the measured differential linear scattering coefficients at different scattering angles for the materials studied in this paper as well as the measured linear attenuation coefficients. Tables A2 and A3 give the measured form factors. The form factors can be used to construct scattering cross sections for any combination of scattering angle and energy. All results in these tables represent the mean values of repeated measurements.

Table A1. Measured scattering coefficients μ_s (from equation (7)) and linear attenuation coefficients μ_t for the materials studied. The subscripts give an upper bound on the percentage uncertainty for each measurement.

Energy	Differential linear scattering coefficient μ_s (cm^{-1} sr^{-1})							μ_t
(keV)	1.7°	3.2°	5.0°	6.3°	10.1°	12.6°	15.1°	(cm^{-1})
				Water				
30	0.0166_{10}	0.0261_5	0.0559_4	0.1221_3	0.1190_5	0.0719_5	0.0534_9	0.365_2
35	0.0168_6	0.0259_6	0.0853_4	0.1723_2	0.0937_5	0.0546_4	0.0519_7	0.305_2
40	0.0169_4	0.0323_4	0.1460_3	0.1537_2	0.0561_4	0.0560_3	0.0458_6	0.271_2
45	0.0159_5	0.0392_5	0.1672_2	0.1244_3	0.0518_6	0.0456_2	0.0385_6	0.243_3
50	0.0165_7	0.0517_4	0.1486_2	0.1179_2	0.0496_6	0.0383_3	0.0356_6	0.230_3
55	0.0162_4	0.0782_3	0.1210_1	0.0971_2	0.0448_4	0.0342_2	0.0341_4	0.223_3
60	0.0195_{13}	0.1082_5	0.1165_3	0.0626_4	0.0371_4	0.0332_7	0.0309_9	0.216_3

Table A1. (Continued.)

Energy	Differential linear scattering coefficient μ_s (cm^{-1} sr^{-1})							μ_t
(keV)	1.7°	3.2°	5.0°	6.3°	10.1°	12.6°	15.1°	(cm^{-1})
65	0.0185_{8}	0.1395_{5}	0.1128_{4}	0.0502_{2}	0.0329_{6}	0.0318_{4}	0.0300_{8}	0.206_{3}
70	0.0208_{6}	0.1425_{4}	0.0894_{6}	0.0496_{5}	0.0306_{5}	0.0324_{4}	0.0316_{8}	0.209_{3}
75	0.0236_{12}	0.1411_{4}	0.0638_{3}	0.0508_{5}	0.0316_{5}	0.0334_{5}	0.0316_{7}	0.195_{4}
80	0.0285_{8}	0.1268_{2}	0.0490_{4}	0.0479_{5}	0.0312_{3}	0.0308_{2}	0.0287_{3}	0.192_{4}
85	0.0348_{8}	0.1167_{5}	0.0487_{2}	0.0446_{8}	0.0302_{2}	0.0348_{5}	0.0309_{8}	0.190_{4}
90	0.0321_{8}	0.1062_{3}	0.0466_{3}	0.0386_{7}	0.0281_{4}	0.0264_{5}	0.0261_{8}	0.192_{4}
95	0.0406_{6}	0.1034_{3}	0.0488_{6}	0.0341_{5}	0.0269_{4}	0.0251_{5}	0.0285_{7}	0.194_{4}
100	0.0471_{9}	0.0885_{3}	0.0447_{5}	0.0306_{7}	0.0248_{3}	0.0247_{10}	0.0213_{7}	0.175_{5}
105	0.0568_{12}	0.0872_{9}	0.0458_{7}	0.0319_{14}	0.0240_{6}	0.0264_{9}	0.0221_{12}	0.188_{6}
110	0.0645_{11}	0.0590_{4}	0.0300_{9}	0.0225_{15}	0.0215_{14}	0.0195_{13}	0.0153_{16}	0.174_{8}
				Polyethylene				
30	0.0120_{11}	0.0196_{2}	0.1007_{3}	0.3381_{7}	0.0483_{5}	0.0405_{4}	0.0365_{6}	0.261_{3}
35	0.0099_{8}	0.0252_{6}	0.5212_{3}	0.0261_{7}	0.0387_{4}	0.0388_{3}	0.0333_{2}	0.228_{3}
40	0.0108_{8}	0.0386_{3}	0.0409_{4}	0.0230_{2}	0.0457_{6}	0.0320_{4}	0.0360_{3}	0.216_{3}
45	0.0113_{6}	0.0734_{4}	0.0248_{3}	0.0526_{4}	0.0317_{5}	0.0414_{3}	0.0329_{2}	0.210_{3}
50	0.0128_{5}	0.1489_{6}	0.0220_{4}	0.0644_{6}	0.0323_{3}	0.0340_{2}	0.0315_{3}	0.203_{3}
55	0.0142_{6}	0.3788_{3}	0.0284_{4}	0.0417_{4}	0.0399_{4}	0.0304_{4}	0.0307_{3}	0.197_{3}
60	0.0161_{4}	0.1693_{6}	0.0355_{6}	0.0318_{6}	0.0302_{2}	0.0280_{6}	0.0301_{3}	0.191_{3}
65	0.0175_{6}	0.0244_{6}	0.0586_{3}	0.0469_{3}	0.0284_{5}	0.0271_{6}	0.0301_{4}	0.189_{3}
70	0.0242_{6}	0.0230_{7}	0.0326_{3}	0.0320_{3}	0.0303_{4}	0.0284_{4}	0.0314_{4}	0.190_{4}
75	0.0353_{7}	0.0268_{5}	0.0331_{4}	0.0328_{7}	0.0285_{5}	0.0302_{5}	0.0296_{8}	0.188_{4}
80	0.0402_{8}	0.0178_{6}	0.0385_{6}	0.0279_{3}	0.0280_{6}	0.0264_{4}	0.0280_{6}	0.173_{4}
85	0.0632_{5}	0.0248_{6}	0.0356_{5}	0.0334_{18}	0.0290_{4}	0.0295_{4}	0.0318_{7}	0.175_{4}
90	0.0856_{5}	0.0343_{7}	0.0286_{4}	0.0349_{5}	0.0289_{4}	0.0271_{6}	0.0260_{6}	0.180_{4}
95	0.1624_{8}	0.0429_{7}	0.0263_{8}	0.0273_{9}	0.0267_{6}	0.0245_{6}	0.0257_{5}	0.170_{5}
100	0.2361_{6}	0.0514_{6}	0.0260_{10}	0.0297_{6}	0.0223_{1}	0.0231_{7}	0.0238_{4}	0.175_{5}
105	0.2496_{5}	0.0427_{7}	0.0243_{8}	0.0263_{10}	0.0229_{4}	0.0209_{10}	0.0265_{3}	0.152_{7}
110	0.1978_{6}	0.0283_{6}	0.0265_{11}	0.0230_{7}	0.0193_{7}	0.0186_{11}	0.0204_{11}	0.164_{9}
				Polystyrene				
30	0.0498_{23}	0.1155_{20}	0.2857_{15}	0.1145_{15}	0.0595_{11}	0.0485_{12}	0.0429_{13}	0.268_{4}
35	0.0683_{23}	0.1225_{20}	0.1887_{15}	0.0701_{15}	0.0607_{10}	0.0442_{11}	0.0395_{12}	0.254_{3}
40	0.0902_{23}	0.1580_{20}	0.0961_{15}	0.0631_{15}	0.0451_{10}	0.0395_{11}	0.0425_{12}	0.222_{4}
45	0.1110_{23}	0.2379_{20}	0.0671_{16}	0.0531_{15}	0.0387_{11}	0.0426_{11}	0.0400_{12}	0.224_{4}
50	0.1156_{23}	0.2413_{20}	0.0580_{16}	0.0586_{14}	0.0364_{11}	0.0441_{11}	0.0339_{12}	0.214_{4}
55	0.1125_{23}	0.1567_{20}	0.0559_{16}	0.0612_{14}	0.0411_{10}	0.0363_{11}	0.0340_{12}	0.205_{4}
60	0.1056_{23}	0.1061_{20}	0.0537_{16}	0.0483_{16}	0.0436_{11}	0.0303_{12}	0.0300_{14}	0.212_{4}
65	0.1081_{23}	0.0698_{20}	0.0593_{16}	0.0404_{15}	0.0408_{11}	0.0311_{12}	0.0335_{12}	0.197_{4}
70	0.1177_{23}	0.0588_{21}	0.0563_{17}	0.0421_{17}	0.0361_{12}	0.0358_{13}	0.0277_{15}	0.200_{5}
75	0.1485_{23}	0.0497_{21}	0.0515_{17}	0.0387_{17}	0.0394_{12}	0.0432_{13}	0.0352_{14}	0.201_{5}
80	0.1608_{23}	0.0461_{21}	0.0379_{18}	0.0318_{18}	0.0283_{12}	0.0355_{13}	0.0339_{14}	0.187_{6}
85	0.2010_{23}	0.0459_{21}	0.0338_{19}	0.0385_{18}	0.0310_{12}	0.0367_{13}	0.0324_{15}	0.184_{6}
90	0.2029_{23}	0.0486_{21}	0.0350_{19}	0.0377_{18}	0.0290_{13}	0.0367_{13}	0.0301_{15}	0.175_{6}
95	0.1888_{23}	0.0482_{22}	0.0277_{20}	0.0348_{19}	0.0297_{13}	0.0320_{14}	0.0252_{17}	0.176_{7}
100	0.1791_{23}	0.0512_{22}	0.0295_{22}	0.0451_{20}	0.0343_{14}	0.0277_{17}	0.0330_{17}	0.199_{7}

Table A1. (Continued.)

Energy (keV)	Differential linear scattering coefficient μ_s (cm^{-1} sr^{-1}) 1.7°	3.2°	5.0°	6.3°	10.1°	12.6°	15.1°	μ_t (cm^{-1})
105	0.1366_{24}	0.0471_{24}	0.0369_{23}	0.0391_{23}	0.0296_{17}	0.0309_{18}	0.0271_{21}	0.206_{8}
110	0.0939_{26}	0.0493_{27}	0.0145_{41}	0.0343_{31}	0.0233_{24}	0.0191_{29}	0.0363_{25}	0.193_{12}
				Polycarbonate				
30	0.0578_{23}	0.1183_{20}	0.2752_{15}	0.1603_{15}	0.0740_{11}	0.0688_{12}	0.0527_{13}	0.330_{3}
35	0.0588_{23}	0.1606_{20}	0.1550_{15}	0.1041_{15}	0.0798_{10}	0.0486_{12}	0.0515_{12}	0.290_{3}
40	0.0677_{23}	0.2921_{20}	0.1396_{15}	0.0774_{15}	0.0593_{10}	0.0476_{11}	0.0570_{12}	0.265_{3}
45	0.0619_{23}	0.2783_{20}	0.0978_{15}	0.0639_{15}	0.0479_{11}	0.0540_{11}	0.0535_{12}	0.251_{3}
50	0.0674_{23}	0.2218_{20}	0.0771_{16}	0.0718_{14}	0.0441_{11}	0.0513_{11}	0.0480_{12}	0.245_{3}
55	0.0670_{23}	0.1446_{20}	0.0627_{16}	0.0710_{14}	0.0423_{11}	0.0458_{11}	0.0396_{12}	0.222_{4}
60	0.0921_{23}	0.1108_{20}	0.0644_{16}	0.0616_{15}	0.0484_{11}	0.0400_{12}	0.0353_{13}	0.225_{4}
65	0.1224_{23}	0.1112_{20}	0.0743_{16}	0.0502_{15}	0.0449_{11}	0.0374_{11}	0.0385_{12}	0.214_{4}
70	0.1718_{23}	0.0869_{20}	0.0696_{17}	0.0509_{16}	0.0409_{12}	0.0364_{13}	0.0410_{14}	0.224_{5}
75	0.2188_{23}	0.0723_{20}	0.0642_{17}	0.0440_{17}	0.0427_{12}	0.0384_{13}	0.0394_{14}	0.197_{5}
80	0.2931_{23}	0.0705_{21}	0.0536_{17}	0.0404_{18}	0.0424_{12}	0.0400_{13}	0.0402_{14}	0.222_{5}
85	0.2777_{23}	0.0574_{21}	0.0431_{18}	0.0405_{18}	0.0413_{12}	0.0395_{13}	0.0393_{14}	0.201_{6}
90	0.2384_{23}	0.0490_{21}	0.0386_{19}	0.0376_{18}	0.0374_{13}	0.0393_{13}	0.0259_{16}	0.199_{6}
95	0.1965_{23}	0.0522_{22}	0.0350_{20}	0.0459_{18}	0.0368_{13}	0.0383_{14}	0.0301_{16}	0.188_{7}
100	0.1684_{23}	0.0556_{22}	0.0377_{21}	0.0553_{19}	0.0352_{14}	0.0257_{17}	0.0276_{19}	0.194_{8}
105	0.1105_{24}	0.0625_{22}	0.0249_{25}	0.0376_{22}	0.0238_{17}	0.0282_{18}	0.0248_{21}	0.156_{10}
110	0.1251_{26}	0.0543_{27}	0.0309_{31}	0.0221_{37}	0.0323_{21}	0.0268_{25}	0.0274_{28}	0.225_{10}
				Nylon				
30	0.0248_{24}	0.0531_{21}	0.2228_{16}	0.3623_{14}	0.0834_{11}	0.0663_{12}	0.0594_{13}	0.327_{3}
35	0.0196_{24}	0.0642_{20}	0.2324_{15}	0.0697_{15}	0.0651_{11}	0.0512_{11}	0.0504_{12}	0.291_{3}
40	0.0219_{24}	0.0885_{20}	0.1399_{15}	0.0610_{15}	0.0562_{10}	0.0490_{11}	0.0590_{12}	0.263_{3}
45	0.0266_{23}	0.1313_{20}	0.0686_{16}	0.0596_{15}	0.0485_{10}	0.0504_{11}	0.0458_{12}	0.246_{3}
50	0.0337_{23}	0.3410_{20}	0.0596_{16}	0.0784_{14}	0.0412_{11}	0.0458_{11}	0.0447_{12}	0.238_{3}
55	0.0409_{23}	0.2443_{20}	0.0585_{16}	0.0682_{15}	0.0411_{11}	0.0445_{11}	0.0422_{12}	0.229_{4}
60	0.0456_{23}	0.2524_{20}	0.0816_{16}	0.0665_{15}	0.0459_{11}	0.0362_{12}	0.0398_{13}	0.234_{3}
65	0.0562_{23}	0.0821_{20}	0.0740_{16}	0.0561_{15}	0.0422_{11}	0.0355_{12}	0.0399_{12}	0.224_{4}
70	0.0610_{23}	0.0549_{21}	0.0683_{17}	0.0347_{18}	0.0377_{12}	0.0397_{13}	0.0410_{14}	0.234_{4}
75	0.0844_{23}	0.0563_{21}	0.0561_{17}	0.0477_{17}	0.0366_{12}	0.0486_{13}	0.0386_{14}	0.213_{5}
80	0.0963_{23}	0.0540_{21}	0.0563_{17}	0.0457_{17}	0.0341_{12}	0.0390_{13}	0.0427_{14}	0.208_{5}
85	0.1248_{23}	0.0608_{21}	0.0511_{18}	0.0427_{18}	0.0389_{12}	0.0448_{13}	0.0340_{15}	0.206_{6}
90	0.1722_{23}	0.0668_{21}	0.0383_{19}	0.0391_{18}	0.0333_{13}	0.0344_{14}	0.0359_{15}	0.209_{6}
95	0.2131_{23}	0.0684_{21}	0.0409_{19}	0.0486_{18}	0.0314_{13}	0.0355_{14}	0.0335_{16}	0.193_{7}
100	0.2282_{23}	0.0570_{22}	0.0388_{21}	0.0336_{21}	0.0282_{15}	0.0251_{17}	0.0405_{16}	0.193_{8}
105	0.2339_{24}	0.0646_{23}	0.0327_{25}	0.0383_{24}	0.0266_{17}	0.0336_{18}	0.0384_{19}	0.216_{8}
110	0.1958_{25}	0.0692_{26}	0.0502_{26}	0.0400_{30}	0.0284_{22}	0.0259_{26}	0.0523_{22}	0.229_{10}
				Fat				
30	0.0659_{3}	0.0447_{8}	0.2544_{10}	0.1402_{6}	0.0700_{10}	0.0538_{14}	0.0403_{13}	0.282_{3}
35	0.0398_{9}	0.0541_{9}	0.2113_{2}	0.0772_{4}	0.0596_{4}	0.0402_{7}	0.0410_{2}	0.242_{3}
40	0.0291_{7}	0.0888_{5}	0.0884_{4}	0.0607_{7}	0.0484_{1}	0.0381_{3}	0.0366_{1}	0.219_{3}
45	0.0284_{9}	0.1497_{5}	0.0658_{2}	0.0586_{6}	0.0377_{2}	0.0393_{2}	0.0320_{3}	0.201_{3}
50	0.0315_{12}	0.2183_{2}	0.0612_{6}	0.0590_{7}	0.0370_{3}	0.0352_{8}	0.0302_{4}	0.189_{3}

Table A1. (Continued.)

Energy	Differential linear scattering coefficient μ_s (cm^{-1} sr^{-1})							μ_t
(keV)	1.7°	3.2°	5.0°	6.3°	10.1°	12.6°	15.1°	(cm^{-1})
55	0.0296_2	0.1803_5	0.0584_1	0.0590_1	0.0385_3	0.0317_4	0.0296_7	0.183_3
60	0.0364_4	0.1123_5	0.0672_7	0.0448_{12}	0.0385_{11}	0.0309_{12}	0.0289_2	0.193_3
65	0.0399_8	0.0714_8	0.0683_2	0.0419_1	0.0353_1	0.0306_6	0.0318_{13}	0.182_4
70	0.0497_7	0.0617_{18}	0.0557_1	0.0385_{11}	0.0285_4	0.0288_3	0.0267_7	0.183_4
75	0.0719_5	0.0575_2	0.0459_8	0.0349_8	0.0320_4	0.0294_1	0.0275_7	0.169_5
80	0.0833_4	0.0548_5	0.0366_9	0.0336_{17}	0.0331_1	0.0267_7	0.0295_5	0.168_5
85	0.1313_6	0.0515_2	0.0395_{12}	0.0327_2	0.0301_2	0.0269_7	0.0258_6	0.172_5
90	0.1459_4	0.0504_1	0.0340_{21}	0.0262_1	0.0285_3	0.0243_3	0.0243_4	0.164_6
95	0.1684_7	0.0510_3	0.0303_7	0.0310_{16}	0.0262_6	0.0226_6	0.0218_5	0.162_6
100	0.1706_2	0.0568_2	0.0313_1	0.0292_1	0.0250_4	0.0249_8	0.0243_2	0.167_7
105	0.1504_{17}	0.0518_5	0.0374_2	0.0252_{28}	0.0262_7	0.0250_{22}	0.0236_{28}	0.171_8
110	0.1420_{12}	0.0422_6	0.0329_1	0.0234_{12}	0.0190_{25}	0.0207_6	0.0233_{16}	0.173_{11}
				Muscle				
30	0.0499_{13}	0.0425_8	0.1009_8	0.1540_4	0.1241_3	0.0707_3	0.0618_9	0.407_2
35	0.0465_{10}	0.0419_2	0.1189_4	0.1685_8	0.0959_4	0.0595_7	0.0602_7	0.341_2
40	0.0453_{13}	0.0500_3	0.1490_8	0.1489_5	0.0615_6	0.0580_3	0.0473_8	0.300_2
45	0.0426_{10}	0.0707_5	0.1724_5	0.1253_9	0.0570_3	0.0543_6	0.0441_7	0.284_2
50	0.0389_{12}	0.0876_7	0.1485_5	0.1168_8	0.0553_5	0.0443_2	0.0423_9	0.263_2
55	0.0347_7	0.1036_7	0.1210_6	0.0980_{11}	0.0496_6	0.0417_6	0.0408_7	0.251_3
60	0.0347_8	0.1147_3	0.1176_9	0.0749_3	0.0447_{10}	0.0359_5	0.0367_{11}	0.242_3
65	0.0336_4	0.1396_7	0.1090_4	0.0576_7	0.0379_5	0.0355_8	0.0348_{12}	0.230_3
70	0.0400_6	0.1558_{11}	0.0911_6	0.0586_8	0.0416_{10}	0.0400_{13}	0.0425_6	0.235_3
75	0.0492_3	0.1472_6	0.0757_7	0.0633_8	0.0425_{11}	0.0397_9	0.0398_{14}	0.241_3
80	0.0481_3	0.1218_5	0.0567_8	0.0563_7	0.0384_{12}	0.0361_9	0.0363_8	0.218_3
85	0.0597_6	0.1145_8	0.0511_{12}	0.0482_8	0.0381_9	0.0346_{11}	0.0358_{13}	0.211_4
90	0.0587_7	0.1050_8	0.0539_{11}	0.0481_8	0.0350_{13}	0.0291_7	0.0321_{11}	0.222_4
95	0.0674_{11}	0.1021_{11}	0.0502_{11}	0.0429_{11}	0.0320_{10}	0.0287_{12}	0.0329_6	0.210_4
100	0.0769_4	0.0940_{12}	0.0513_{11}	0.0481_{12}	0.0355_{13}	0.0334_{17}	0.0292_{17}	0.222_4
105	0.0982_{14}	0.0969_{12}	0.0550_8	0.0456_9	0.0343_{17}	0.0275_{16}	0.0313_{18}	0.247_5
110	0.1037_{14}	0.0801_7	0.0546_{23}	0.0374_{12}	0.0354_5	0.0241_{25}	0.0229_{17}	0.239_7
				Liver				
30	0.0535_6	0.0520_6	0.0966_6	0.1502_7	0.1303_{10}	0.0807_{11}	0.0687_{14}	0.410_2
35	0.0488_6	0.0495_{14}	0.1199_{10}	0.1738_8	0.1012_8	0.0601_9	0.0591_8	0.346_2
40	0.0489_6	0.0583_9	0.1560_8	0.1516_{10}	0.0631_8	0.0563_6	0.0509_{10}	0.299_2
45	0.0467_6	0.0745_9	0.1683_9	0.1250_{11}	0.0592_{10}	0.0519_{11}	0.0443_{12}	0.275_2
50	0.0433_5	0.0878_6	0.1484_8	0.1172_6	0.0578_7	0.0454_9	0.0414_{10}	0.256_3
55	0.0407_5	0.1039_8	0.1255_6	0.0974_8	0.0526_7	0.0411_7	0.0428_6	0.243_3
60	0.0369_6	0.1209_7	0.1239_7	0.0638_6	0.0431_7	0.0376_7	0.0354_{11}	0.233_3
65	0.0389_6	0.1417_4	0.1149_8	0.0552_6	0.0419_4	0.0362_8	0.0337_8	0.229_3
70	0.0407_8	0.1397_8	0.0909_9	0.0552_{12}	0.0391_{11}	0.0370_7	0.0341_{10}	0.227_3
75	0.0518_5	0.1331_6	0.0641_8	0.0531_7	0.0386_3	0.0352_5	0.0365_7	0.212_4
80	0.0490_{11}	0.1139_9	0.0544_8	0.0516_6	0.0369_7	0.0332_{10}	0.0359_{15}	0.208_4
85	0.0610_9	0.1056_5	0.0529_9	0.0411_7	0.0348_5	0.0354_{15}	0.0346_{10}	0.203_4

Table A1. (Continued.)

Energy	Differential linear scattering coefficient μ_s (cm^{-1} sr^{-1})							μ_t
(keV)	1.7°	3.2°	5.0°	6.3°	10.1°	12.6°	15.1°	(cm^{-1})
90	0.0579_{8}	0.0981_{9}	0.0507_{5}	0.0451_{8}	0.0310_{6}	0.0261_{5}	0.0300_{15}	0.202_{4}
95	0.0710_{9}	0.1005_{5}	0.0476_{9}	0.0459_{4}	0.0319_{7}	0.0306_{5}	0.0323_{12}	0.208_{4}
100	0.0735_{11}	0.0963_{7}	0.0464_{10}	0.0346_{15}	0.0292_{16}	0.0269_{5}	0.0276_{17}	0.200_{5}
105	0.0760_{10}	0.0881_{7}	0.0553_{12}	0.0342_{2}	0.0311_{8}	0.0255_{21}	0.0226_{8}	0.200_{6}
110	0.0809_{7}	0.0684_{11}	0.0496_{10}	0.0279_{4}	0.0283_{16}	0.0143_{17}	0.0192_{16}	0.165_{9}
				Kidney				
30	0.0397_{24}	0.0309_{22}	0.0636_{17}	0.1378_{15}	0.1155_{11}	0.0657_{12}	0.0465_{13}	0.389_{3}
35	0.0324_{24}	0.0291_{22}	0.0853_{16}	0.1696_{14}	0.0930_{11}	0.0509_{11}	0.0374_{13}	0.320_{3}
40	0.0342_{24}	0.0402_{21}	0.1278_{15}	0.1321_{14}	0.0553_{11}	0.0482_{11}	0.0406_{12}	0.279_{3}
45	0.0310_{24}	0.0491_{21}	0.1417_{15}	0.1232_{14}	0.0538_{11}	0.0451_{11}	0.0357_{12}	0.257_{3}
50	0.0290_{24}	0.0691_{20}	0.1322_{15}	0.1103_{14}	0.0497_{11}	0.0375_{11}	0.0296_{12}	0.246_{4}
55	0.0257_{24}	0.0776_{20}	0.1105_{15}	0.0886_{14}	0.0467_{11}	0.0331_{11}	0.0294_{12}	0.232_{4}
60	0.0291_{24}	0.0997_{20}	0.0984_{16}	0.0569_{15}	0.0424_{12}	0.0300_{12}	0.0265_{14}	0.218_{4}
65	0.0280_{24}	0.1170_{20}	0.0952_{15}	0.0414_{15}	0.0364_{11}	0.0304_{11}	0.0257_{12}	0.207_{4}
70	0.0307_{25}	0.1211_{20}	0.0804_{16}	0.0438_{16}	0.0376_{12}	0.0278_{13}	0.0257_{14}	0.199_{5}
75	0.0332_{25}	0.1328_{20}	0.0666_{17}	0.0477_{16}	0.0369_{12}	0.0352_{13}	0.0268_{15}	0.220_{5}
80	0.0382_{25}	0.1033_{21}	0.0481_{17}	0.0461_{17}	0.0352_{12}	0.0298_{13}	0.0216_{15}	0.201_{5}
85	0.0490_{25}	0.1085_{21}	0.0420_{18}	0.0268_{20}	0.0315_{13}	0.0295_{13}	0.0184_{16}	0.182_{6}
90	0.0506_{24}	0.0936_{21}	0.0385_{18}	0.0394_{18}	0.0288_{13}	0.0241_{14}	0.0171_{17}	0.193_{6}
95	0.0541_{24}	0.0929_{21}	0.0443_{18}	0.0395_{19}	0.0308_{14}	0.0259_{15}	0.0214_{17}	0.189_{7}
100	0.0530_{25}	0.0794_{21}	0.0414_{19}	0.0312_{21}	0.0256_{15}	0.0195_{17}	0.0199_{19}	0.175_{8}
105	0.0705_{25}	0.0644_{23}	0.0374_{22}	0.0268_{24}	0.0282_{16}	0.0151_{21}	0.0259_{19}	0.166_{10}
110	0.0819_{26}	0.0644_{25}	0.0480_{25}	0.0197_{35}	0.0199_{23}	0.0190_{26}	0.0233_{26}	0.197_{11}
				Bone				
30	0.2420_{25}	0.0759_{27}	0.1939_{26}	0.2256_{26}	0.2817_{23}	0.2473_{23}	0.1494_{29}	2.273_{4}
35	0.2385_{24}	0.0975_{25}	0.2058_{25}	0.2379_{26}	0.2094_{22}	0.1313_{23}	0.1209_{28}	1.696_{4}
40	0.1319_{24}	0.1110_{24}	0.2231_{25}	0.7446_{25}	0.2266_{22}	0.1266_{23}	0.1237_{28}	1.193_{5}
45	0.0977_{24}	0.1137_{24}	0.2596_{24}	0.1554_{25}	0.1485_{22}	0.1419_{23}	0.0990_{28}	0.887_{6}
50	0.1108_{24}	0.1106_{24}	0.6905_{24}	0.2339_{25}	0.1333_{22}	0.1167_{23}	0.0829_{28}	0.738_{6}
55	0.0739_{24}	0.1498_{24}	0.2092_{24}	0.1778_{25}	0.1564_{22}	0.1143_{23}	0.0757_{28}	0.700_{6}
60	0.0600_{26}	0.1770_{24}	0.2324_{25}	0.2495_{25}	0.1282_{22}	0.0942_{23}	0.0684_{29}	0.613_{7}
65	0.0695_{25}	0.1579_{24}	0.1807_{25}	0.1311_{25}	0.1100_{22}	0.0796_{23}	0.0678_{28}	0.465_{9}
70	0.0664_{28}	0.2366_{24}	0.1738_{25}	0.1405_{26}	0.1075_{23}	0.0815_{23}	0.0572_{29}	0.599_{9}
75	0.0917_{28}	0.4200_{23}	0.2237_{25}	0.1522_{26}	0.0946_{23}	0.0906_{23}	0.0694_{29}	0.430_{12}
80	0.0971_{30}	0.5251_{23}	0.2016_{25}	0.1046_{26}	0.0870_{23}	0.0882_{23}	0.0556_{29}	0.358_{15}
85	0.1244_{29}	0.2250_{24}	0.1275_{26}	0.1003_{27}	0.0860_{23}	0.0721_{24}	0.0553_{29}	0.409_{14}
90	0.1047_{26}	0.1411_{25}	0.1478_{26}	0.1083_{27}	0.0754_{23}	0.0662_{24}	0.0583_{29}	0.351_{17}
95	0.1164_{26}	0.1715_{24}	0.1515_{26}	0.1057_{27}	0.0746_{23}	0.0650_{24}	0.0534_{30}	0.294_{22}
100	0.1353_{26}	0.1864_{25}	0.1060_{27}	0.1186_{28}	0.0796_{24}	0.0598_{25}	0.0531_{30}	0.422_{18}
105	0.1110_{28}	0.1275_{26}	0.0844_{29}	0.0620_{31}	0.0491_{25}	0.0592_{26}	0.0405_{32}	0.271_{31}
110	0.0690_{37}	0.1277_{29}	0.1616_{29}	0.1385_{31}	0.0479_{28}	0.0360_{31}	0.0468_{34}	0.177_{66}

Table A2. Measured coherent form factors for water and plastics. The subscripts give an upper bound on the percentage uncertainty for each measurement. The values of F_{inc} in this table were obtained from the composition data of table 2 and the data of Hubbell and Øverbø (1979). They have been used to extract the F_{coh} values and so must also be used to construct scatter cross sections at arbitrary θ. The water and polyethylene data include measurements subsequent to King (2009). The other three plastics are from the same experiments reported in King (2009) but here are on a more detailed x-grid.

x	Water		Polyethylene		Polystyrene		Polycarbonate		Nylon	
(nm^{-1})	F_{coh}	F_{inc}	F_{coh}	F_{inc}	F_{coh}	F_{inc}	F_{coh}	F_{inc}	F_{coh}	F_{inc}
0.363	0.813_4	0.026	0.700_4	0.035	1.422_{12}	0.032	1.306_{12}	0.029	0.825_{13}	0.031
0.378	0.782_4	0.028	0.678_6	0.038	1.449_{12}	0.035	1.365_{12}	0.032	0.824_{13}	0.034
0.386	0.776_5	0.029	0.674_5	0.039	1.423_{12}	0.036	1.333_{12}	0.033	0.824_{13}	0.035
0.402	0.765_4	0.031	0.670_4	0.043	1.555_{12}	0.039	1.394_{12}	0.035	0.773_{13}	0.038
0.410	0.774_4	0.033	0.608_6	0.044	1.575_{12}	0.040	1.417_{12}	0.037	0.807_{13}	0.040
0.419	0.774_3	0.034	0.658_6	0.046	1.630_{12}	0.042	1.468_{12}	0.038	0.796_{13}	0.041
0.436	0.757_4	0.037	0.650_4	0.050	1.690_{12}	0.045	1.416_{12}	0.041	0.786_{13}	0.044
0.445	0.750_3	0.038	0.615_5	0.052	1.721_{12}	0.047	1.459_{12}	0.043	0.771_{13}	0.046
0.463	0.763_4	0.041	0.617_5	0.056	1.810_{12}	0.051	1.432_{12}	0.046	0.817_{13}	0.050
0.473	0.770_3	0.043	0.634_6	0.058	1.827_{12}	0.053	1.474_{12}	0.048	0.823_{13}	0.052
0.492	0.742_2	0.046	0.633_5	0.063	1.938_{12}	0.057	1.447_{12}	0.052	0.826_{13}	0.056
0.502	0.742_3	0.048	0.632_5	0.065	1.957_{12}	0.059	1.437_{12}	0.054	0.845_{13}	0.058
0.513	0.777_2	0.050	0.651_6	0.067	1.967_{12}	0.062	1.454_{12}	0.056	0.884_{13}	0.060
0.523	0.753_3	0.052	0.624_5	0.070	2.005_{12}	0.064	1.415_{12}	0.058	0.882_{13}	0.063
0.545	0.754_4	0.056	0.634_4	0.076	2.023_{12}	0.069	1.478_{12}	0.063	0.940_{13}	0.068
0.556	0.754_3	0.058	0.654_4	0.078	1.991_{12}	0.072	1.441_{12}	0.065	0.934_{13}	0.070
0.579	0.754_5	0.063	0.643_5	0.084	2.048_{12}	0.077	1.468_{12}	0.071	1.006_{12}	0.076
0.591	0.725_6	0.065	0.641_4	0.088	2.042_{12}	0.080	1.488_{12}	0.073	0.989_{13}	0.078
0.615	0.739_4	0.071	0.658_2	0.094	2.008_{12}	0.086	1.469_{12}	0.079	1.055_{12}	0.084
0.628	0.729_4	0.073	0.663_3	0.098	1.986_{12}	0.089	1.521_{12}	0.082	1.076_{12}	0.088
0.653	0.742_3	0.079	0.675_3	0.105	1.970_{12}	0.096	1.585_{12}	0.088	1.078_{13}	0.094
0.667	0.769_4	0.082	0.688_4	0.109	1.880_{12}	0.100	1.620_{12}	0.091	1.142_{13}	0.098
0.694	0.928_3	0.088	0.841_5	0.117	2.061_{10}	0.107	1.977_{11}	0.098	1.296_{11}	0.105
0.709	0.895_4	0.091	0.821_3	0.121	2.058_{10}	0.111	2.019_{11}	0.101	1.288_{11}	0.109
0.738	0.913_5	0.098	0.870_4	0.130	2.028_{10}	0.119	2.043_{10}	0.109	1.419_{11}	0.117
0.753	0.963_2	0.102	0.891_3	0.135	2.011_{10}	0.123	2.187_{10}	0.113	1.490_{11}	0.121
0.784	0.961_3	0.110	0.906_3	0.145	2.124_{10}	0.132	2.397_{10}	0.121	1.472_{11}	0.130
0.800	0.975_3	0.114	0.940_2	0.150	2.132_{10}	0.137	2.526_{10}	0.125	1.434_{11}	0.134
0.833	1.006_2	0.122	0.977_3	0.160	2.136_{10}	0.146	2.742_{10}	0.134	1.561_{11}	0.144
0.850	0.997_3	0.126	1.014_3	0.166	2.268_{10}	0.152	2.907_{10}	0.139	1.572_{11}	0.149
0.885	1.021_2	0.135	1.086_3	0.177	2.359_{10}	0.162	3.111_{10}	0.149	1.668_{11}	0.159
0.903	1.069_3	0.140	1.190_4	0.183	2.429_{10}	0.168	3.170_{10}	0.154	1.707_{11}	0.165
0.940	1.080_2	0.150	1.281_5	0.196	2.627_{10}	0.179	3.227_{10}	0.165	1.744_{11}	0.176
0.960	1.112_2	0.155	1.364_6	0.202	2.711_{10}	0.185	3.220_{10}	0.170	1.831_{11}	0.182
1.00	1.160_2	0.166	1.479_7	0.215	2.883_{10}	0.197	3.080_{10}	0.182	2.036_{11}	0.194
1.02	1.177_3	0.172	1.544_8	0.222	2.961_{10}	0.203	3.054_{10}	0.187	2.222_{10}	0.201
1.06	1.265_2	0.183	1.709_8	0.236	2.978_{10}	0.216	2.896_{10}	0.199	2.949_{10}	0.214
1.08	1.361_3	0.189	1.864_8	0.243	3.198_8	0.223	3.020_8	0.206	2.870_8	0.220
1.11	1.485_4	0.196	1.860_8	0.251	3.149_8	0.230	2.945_8	0.212	3.515_8	0.227
1.13	1.436_2	0.202	2.355_{11}	0.258	3.087_8	0.237	2.848_8	0.219	3.268_{10}	0.234

Table A2. (Continued.)

x	Water		Polyethylene		Polystyrene		Polycarbonate		Nylon	
(nm^{-1})	F_{coh}	F_{inc}	F_{coh}	F_{inc}	F_{coh}	F_{inc}	F_{coh}	F_{inc}	F_{coh}	F_{inc}
1.15	1.523_3	0.208	2.367_{10}	0.266	2.977_8	0.244	2.729_8	0.225	3.582_8	0.241
1.20	1.626_3	0.222	4.781_{18}	0.282	2.772_8	0.258	2.473_8	0.239	2.991_8	0.256
1.22	1.678_3	0.229	3.507_{15}	0.290	2.684_8	0.266	2.323_8	0.246	2.720_8	0.263
1.27	1.763_5	0.243	2.337_9	0.307	2.386_8	0.282	2.246_8	0.261	2.961_8	0.279
1.30	1.914_2	0.250	2.318_6	0.316	2.259_8	0.290	2.239_8	0.269	3.217_8	0.287
1.33	2.017_2	0.258	2.933_9	0.325	2.135_8	0.298	2.082_8	0.277	3.472_8	0.295
1.35	2.107_2	0.266	2.643_7	0.334	1.867_8	0.307	2.190_8	0.285	3.114_7	0.304
1.38	2.219_2	0.273	1.809_6	0.343	1.911_8	0.315	2.119_8	0.293	2.617_8	0.312
1.44	2.434_2	0.289	1.229_{23}	0.361	1.691_8	0.332	2.065_8	0.309	1.714_8	0.329
1.47	2.383_2	0.297	1.233_{24}	0.370	1.769_8	0.341	1.907_8	0.317	1.672_8	0.338
1.53	2.505_1	0.314	1.156_{29}	0.389	1.605_8	0.359	1.811_8	0.334	1.461_9	0.356
1.56	2.528_1	0.323	1.126_{31}	0.399	1.532_9	0.368	1.860_8	0.343	1.396_9	0.365
1.62	2.514_2	0.340	1.174_{28}	0.418	1.405_9	0.386	1.713_8	0.361	1.366_9	0.383
1.66	2.423_1	0.349	1.258_{23}	0.428	1.355_9	0.395	1.678_8	0.369	1.372_9	0.392
1.73	2.381_2	0.366	1.032_{32}	0.447	1.312_9	0.414	1.542_9	0.387	1.294_9	0.411
1.76	2.346_1	0.375	0.968_{35}	0.457	1.347_9	0.423	1.518_9	0.396	1.229_9	0.420
1.80	2.276_1	0.385	0.968_{33}	0.466	1.367_9	0.432	1.495_9	0.405	1.240_9	0.430
1.83	2.214_2	0.394	0.976_{30}	0.476	1.245_9	0.442	1.535_9	0.414	1.284_9	0.439
1.87	2.189_2	0.403	0.958_{32}	0.486	1.235_9	0.451	1.432_9	0.424	1.165_{10}	0.449
1.95	2.093_1	0.422	1.106_{22}	0.505	1.278_9	0.470	1.446_9	0.442	1.221_{10}	0.467
1.99	2.082_1	0.431	1.340_{13}	0.515	1.259_9	0.479	1.336_9	0.451	1.302_9	0.477
2.07	2.030_2	0.450	1.059_{22}	0.534	1.246_{10}	0.498	1.325_9	0.470	1.518_9	0.496
2.11	1.993_2	0.459	1.067_{19}	0.544	1.281_9	0.507	1.357_9	0.479	1.553_9	0.505
2.20	2.031_3	0.478	1.605_5	0.562	1.361_7	0.526	1.480_7	0.497	1.504_7	0.524
2.24	1.983_3	0.487	1.614_5	0.572	1.417_7	0.535	1.548_7	0.507	1.521_7	0.533
2.34	1.933_3	0.506	1.497_6	0.590	1.328_7	0.553	1.509_7	0.525	1.482_7	0.551
2.38	1.887_3	0.515	1.321_9	0.599	1.274_7	0.562	1.507_7	0.534	1.434_7	0.560
2.48	1.713_3	0.534	1.068_{12}	0.616	1.338_7	0.579	1.488_7	0.552	1.347_7	0.578
2.53	1.652_3	0.543	1.129_9	0.625	1.306_7	0.588	1.518_7	0.560	1.350_7	0.587
2.64	1.444_3	0.561	1.016_9	0.641	1.139_8	0.605	1.387_7	0.577	1.221_7	0.604
2.69	1.392_3	0.570	1.023_9	0.649	1.092_9	0.613	1.334_8	0.586	1.288_8	0.612
2.80	1.318_2	0.588	1.053_6	0.665	1.069_9	0.629	1.258_8	0.602	1.212_8	0.628
2.86	1.281_4	0.597	1.245_4	0.673	0.951_{10}	0.637	1.243_8	0.611	1.228_8	0.636
2.98	1.221_2	0.614	1.099_5	0.687	0.950_{10}	0.652	1.141_8	0.626	1.193_8	0.652
3.04	1.251_2	0.622	0.959_9	0.694	0.980_9	0.659	1.065_9	0.634	1.151_8	0.659
3.17	1.225_3	0.638	0.845_9	0.706	0.929_{10}	0.672	1.108_9	0.648	1.021_9	0.672
3.23	1.195_5	0.646	0.929_8	0.712	1.044_{10}	0.678	1.025_{11}	0.655	1.082_{10}	0.679
3.36	1.232_6	0.662	0.966_{10}	0.724	1.049_{10}	0.691	1.108_{10}	0.668	1.134_{10}	0.692
3.43	1.219_6	0.669	0.964_5	0.730	1.000_{10}	0.697	1.067_{10}	0.675	1.039_{10}	0.698
3.57	1.224_4	0.684	0.944_7	0.741	0.930_{11}	0.708	1.112_9	0.687	1.141_9	0.710
3.65	1.181_5	0.691	0.850_7	0.746	1.002_{10}	0.714	1.111_9	0.694	0.977_{11}	0.716
3.80	1.121_3	0.705	0.924_5	0.757	0.988_{10}	0.725	1.106_9	0.706	1.036_{10}	0.728
3.88	1.066_6	0.712	0.922_5	0.762	0.992_{10}	0.730	1.010_{10}	0.711	0.986_{10}	0.733
3.95	1.042_4	0.719	0.970_3	0.766	0.879_{11}	0.735	1.043_{10}	0.717	1.070_{10}	0.739
4.04	1.066_6	0.725	1.007_3	0.771	0.951_{11}	0.740	1.127_9	0.722	1.210_9	0.743

Table A2. (Continued.)

x	Water		Polyethylene		Polystyrene		Polycarbonate		Nylon	
(nm^{-1})	F_{coh}	F_{inc}	F_{coh}	F_{inc}	F_{coh}	F_{inc}	F_{coh}	F_{inc}	F_{coh}	F_{inc}
4.12	1.022_5	0.731	0.992_2	0.774	1.073_{10}	0.744	1.172_9	0.727	1.115_9	0.748
4.29	0.953_6	0.742	0.802_2	0.782	1.010_{10}	0.752	1.066_{10}	0.736	1.088_9	0.757
4.38	0.943_3	0.748	0.822_3	0.785	0.997_{10}	0.756	1.107_9	0.741	1.019_{10}	0.761
4.56	0.891_6	0.759	0.864_3	0.793	0.952_{11}	0.764	1.100_9	0.750	1.048_{10}	0.769
4.65	0.880_6	0.764	0.770_6	0.796	0.920_{11}	0.768	1.078_9	0.754	0.978_{10}	0.773
4.84	0.811_6	0.774	0.734_3	0.803	0.835_{12}	0.776	0.998_{10}	0.763	0.967_{10}	0.781
4.94	0.789_6	0.779	0.741_2	0.807	0.851_{12}	0.780	1.003_{10}	0.767	0.883_{11}	0.785
5.14	0.763_7	0.788	0.718_3	0.813	0.785_{13}	0.787	0.905_{11}	0.775	0.847_{12}	0.793
5.25	0.784_7	0.792	0.674_5	0.816	0.720_{14}	0.790	0.907_{11}	0.778	0.839_{12}	0.796
5.47	0.727_5	0.800	0.660_4	0.822	0.742_{14}	0.797	0.853_{12}	0.786	0.856_{12}	0.803
5.58	0.739_5	0.804	0.671_5	0.825	0.703_{15}	0.800	0.839_{12}	0.789	0.827_{12}	0.806
5.81	0.707_8	0.811	0.614_4	0.831	0.749_{14}	0.807	0.744_{14}	0.797	0.813_{13}	0.813
5.93	0.709_7	0.815	0.628_3	0.834	0.656_{16}	0.811	0.785_{13}	0.800	0.747_{14}	0.816
6.17	0.533_8	0.822	0.488_{13}	0.840	0.596_{17}	0.817	0.701_{14}	0.808	0.631_{16}	0.823
6.30	0.633_5	0.825	0.598_4	0.843	0.666_{15}	0.821	0.682_{15}	0.811	0.619_{17}	0.826
6.56	0.565_{10}	0.831	0.593_3	0.849	0.719_{15}	0.828	0.669_{16}	0.818	0.716_{15}	0.833
6.69	0.573_{11}	0.834	0.626_2	0.852	0.680_{16}	0.832	0.692_{15}	0.822	0.782_{13}	0.836
6.97	0.621_9	0.840	0.632_3	0.859	0.723_{15}	0.839	0.716_{15}	0.830	0.637_{22}	0.843
7.11	0.603_5	0.843	0.507_5	0.862	0.721_{14}	0.842	0.670_{15}	0.833	0.743_{14}	0.846
7.40	0.589_5	0.849	0.559_7	0.869	0.720_{14}	0.850	0.548_{34}	0.841	0.687_{15}	0.853
7.87	0.615_7	0.857	0.600_5	0.879	0.729_{16}	0.861	0.703_{16}	0.852	0.718_{16}	0.863
8.03	0.560_{10}	0.860	0.569_5	0.882	0.663_{25}	0.865	0.782_{14}	0.856	0.751_{15}	0.867
8.70	0.557_9	0.871	0.562_4	0.895	0.690_{17}	0.880	0.726_{15}	0.871	0.656_{18}	0.881
9.25	0.453_8	0.879	0.505_8	0.906	0.650_{18}	0.892	0.669_{17}	0.883	0.666_{18}	0.891

Table A3. Measured coherent form factors for tissues. The subscripts and values for F_{inc} have the meanings given in table A2. The fat data include measurements subsequent to King (2009).

x	Fat		Muscle		Liver		Kidney		Bone	
(nm^{-1})	F_{coh}	F_{inc}	F_{coh}	F_{inc}	F_{coh}	F_{inc}	F_{coh}	F_{inc}	F_{coh}	F_{inc}
0.363	1.579_4	0.032	1.290_8	0.026	1.400_3	0.027	1.177_{13}	0.027	2.188_{12}	0.028
0.378	1.525_5	0.035	1.298_5	0.029	1.359_4	0.029	1.152_{12}	0.029	2.448_{12}	0.030
0.386	1.459_4	0.036	1.274_5	0.030	1.332_4	0.030	1.038_{13}	0.030	2.424_{12}	0.032
0.402	1.297_3	0.039	1.324_6	0.032	1.350_2	0.033	1.149_{12}	0.032	2.263_{12}	0.034
0.410	1.237_5	0.040	1.287_6	0.033	1.330_2	0.034	1.090_{12}	0.034	2.252_{12}	0.035
0.419	1.154_4	0.042	1.288_6	0.035	1.320_5	0.036	1.082_{12}	0.035	2.164_{12}	0.037
0.436	1.151_4	0.045	1.250_7	0.037	1.347_4	0.038	1.098_{12}	0.038	1.998_{12}	0.039
0.445	1.110_4	0.047	1.248_7	0.039	1.325_4	0.040	1.077_{12}	0.039	1.927_{12}	0.041
0.463	1.087_5	0.051	1.254_6	0.042	1.295_4	0.043	1.064_{12}	0.042	1.768_{12}	0.044
0.473	1.084_5	0.053	1.278_7	0.044	1.312_4	0.045	1.068_{12}	0.044	1.729_{12}	0.046
0.492	1.076_6	0.057	1.222_7	0.047	1.302_2	0.049	1.043_{12}	0.048	1.504_{12}	0.049
0.502	1.077_7	0.059	1.221_6	0.049	1.318_4	0.050	1.043_{12}	0.050	1.541_{12}	0.051
0.513	1.061_4	0.062	1.231_6	0.051	1.262_2	0.052	1.072_{12}	0.051	1.481_{12}	0.053

Table A3. (Continued.)

x	Fat		Muscle		Liver		Kidney		Bone	
(nm^{-1})	F_{coh}	F_{inc}	F_{coh}	F_{inc}	F_{coh}	F_{inc}	F_{coh}	F_{inc}	F_{coh}	F_{inc}
0.523	1.056_5	0.064	1.231_7	0.053	1.273_5	0.054	1.067_{12}	0.053	1.454_{12}	0.055
0.545	1.043_3	0.069	1.198_6	0.057	1.266_3	0.059	1.021_{13}	0.058	1.419_{12}	0.059
0.556	1.070_4	0.072	1.225_5	0.059	1.256_2	0.061	1.052_{12}	0.060	1.374_{13}	0.061
0.579	1.107_4	0.077	1.165_6	0.064	1.235_3	0.066	1.024_{13}	0.065	1.438_{12}	0.065
0.591	1.079_2	0.080	1.138_7	0.067	1.238_4	0.068	0.973_{13}	0.067	1.488_{12}	0.067
0.615	1.096_4	0.086	1.128_4	0.072	1.193_2	0.074	0.995_{13}	0.072	1.412_{12}	0.072
0.628	1.059_2	0.089	1.125_5	0.074	1.169_4	0.076	0.964_{13}	0.075	1.369_{12}	0.075
0.653	1.101_6	0.096	1.089_4	0.080	1.165_2	0.082	0.922_{13}	0.081	1.261_{13}	0.080
0.667	1.109_5	0.100	1.109_4	0.083	1.151_4	0.085	0.975_{13}	0.084	1.192_{13}	0.083
0.694	1.270_7	0.107	1.225_6	0.089	1.310_5	0.092	1.021_{12}	0.090	1.374_{14}	0.088
0.709	1.345_6	0.111	1.207_3	0.093	1.289_2	0.095	1.062_{12}	0.094	1.439_{14}	0.091
0.738	1.382_9	0.119	1.144_4	0.100	1.264_7	0.102	1.050_{12}	0.101	1.319_{14}	0.097
0.753	1.393_7	0.123	1.216_4	0.103	1.293_5	0.106	1.033_{12}	0.104	1.407_{13}	0.101
0.784	1.438_6	0.132	1.205_4	0.111	1.307_3	0.114	0.978_{12}	0.112	1.433_{13}	0.107
0.800	1.469_7	0.137	1.258_4	0.115	1.304_4	0.118	1.022_{12}	0.116	1.492_{13}	0.111
0.833	1.562_3	0.147	1.257_6	0.124	1.313_4	0.127	1.072_{12}	0.125	1.494_{13}	0.118
0.850	1.630_5	0.152	1.267_4	0.128	1.350_5	0.131	1.018_{12}	0.129	1.503_{13}	0.122
0.885	1.814_3	0.163	1.316_3	0.137	1.392_4	0.141	1.121_{12}	0.138	1.563_{13}	0.129
0.903	1.930_4	0.168	1.359_3	0.142	1.395_6	0.146	1.087_{12}	0.143	1.608_{13}	0.133
0.940	2.112_3	0.180	1.428_3	0.152	1.463_5	0.156	1.153_{12}	0.153	1.558_{13}	0.142
0.960	2.199_2	0.186	1.449_2	0.157	1.517_4	0.161	1.231_{12}	0.158	1.576_{13}	0.146
1.00	2.377_3	0.198	1.551_3	0.168	1.568_5	0.172	1.334_{11}	0.169	1.618_{13}	0.155
1.02	2.534_2	0.204	1.552_3	0.174	1.597_5	0.178	1.316_{11}	0.175	1.544_{13}	0.160
1.06	2.909_1	0.218	1.683_3	0.185	1.663_4	0.190	1.362_{11}	0.187	1.646_{13}	0.169
1.08	3.243_2	0.224	1.876_4	0.191	1.880_3	0.196	1.645_9	0.193	2.075_{14}	0.174
1.11	3.283_1	0.231	1.863_3	0.198	1.863_4	0.203	1.582_9	0.199	1.993_{14}	0.179
1.13	3.207_4	0.238	1.940_6	0.204	1.853_3	0.209	1.632_9	0.206	2.020_{14}	0.184
1.15	3.147_2	0.246	1.943_4	0.210	1.931_6	0.216	1.603_9	0.212	1.956_{14}	0.190
1.20	2.966_3	0.261	1.998_4	0.224	1.970_5	0.229	1.683_9	0.226	2.044_{13}	0.200
1.22	2.866_1	0.268	1.995_3	0.231	1.990_5	0.236	1.699_9	0.233	1.997_{13}	0.206
1.27	2.835_2	0.284	2.102_2	0.245	2.098_6	0.251	1.830_8	0.247	2.090_{13}	0.218
1.30	2.713_2	0.292	2.153_4	0.252	2.136_4	0.259	1.820_8	0.254	2.043_{13}	0.224
1.33	2.447_3	0.301	2.147_4	0.260	2.144_4	0.266	1.983_8	0.262	2.003_{13}	0.230
1.35	2.147_5	0.309	2.294_2	0.268	2.283_5	0.274	2.050_8	0.270	2.134_{14}	0.236
1.38	1.996_5	0.318	2.376_2	0.275	2.263_5	0.282	2.184_8	0.277	2.299_{14}	0.242
1.44	1.836_3	0.335	2.356_4	0.291	2.390_5	0.298	2.281_8	0.293	2.458_{14}	0.255
1.47	1.782_3	0.344	2.376_4	0.299	2.399_5	0.306	2.212_8	0.302	2.265_{14}	0.262
1.53	1.696_1	0.362	2.429_5	0.316	2.455_4	0.323	2.279_8	0.318	2.224_{14}	0.275
1.56	1.646_4	0.371	2.441_4	0.325	2.436_5	0.332	2.444_8	0.327	2.317_{14}	0.282
1.62	1.561_3	0.390	2.458_6	0.342	2.410_4	0.349	2.317_8	0.344	2.503_{13}	0.297
1.66	1.433_4	0.399	2.374_5	0.351	2.364_5	0.358	2.365_8	0.353	2.584_{13}	0.304
1.73	1.444_4	0.418	2.280_3	0.368	2.260_4	0.376	2.223_8	0.371	3.539_{13}	0.318

Table A3. (Continued.)

x	Fat		Muscle		Liver		Kidney		Bone	
(nm^{-1})	F_{coh}	F_{inc}	F_{coh}	F_{inc}	F_{coh}	F_{inc}	F_{coh}	F_{inc}	F_{coh}	F_{inc}
1.76	1.429_4	0.427	2.296_3	0.377	2.279_5	0.385	2.078_8	0.380	4.087_{13}	0.326
1.80	1.375_5	0.437	2.219_4	0.386	2.222_5	0.394	2.035_8	0.389	3.989_{13}	0.333
1.83	1.365_4	0.446	2.203_4	0.396	2.127_5	0.404	2.057_8	0.398	3.382_{13}	0.341
1.87	1.432_3	0.456	2.154_4	0.405	2.097_4	0.413	1.967_8	0.407	2.812_{13}	0.349
1.95	1.405_3	0.475	2.103_4	0.423	2.041_4	0.431	1.951_8	0.426	2.065_{14}	0.364
1.99	1.380_4	0.484	2.070_4	0.433	2.030_5	0.441	2.020_8	0.435	1.862_{14}	0.372
2.07	1.417_3	0.503	2.026_4	0.451	2.032_3	0.460	1.858_8	0.454	1.865_{14}	0.388
2.11	1.383_3	0.513	2.010_4	0.461	1.996_4	0.469	1.878_8	0.463	1.940_{14}	0.396
2.20	1.513_3	0.531	2.021_4	0.479	2.084_5	0.488	2.002_6	0.482	2.560_{12}	0.412
2.24	1.533_3	0.541	2.059_4	0.489	2.036_4	0.497	1.892_6	0.491	2.464_{12}	0.420
2.34	1.541_3	0.559	1.913_4	0.507	1.913_6	0.516	1.842_6	0.510	2.079_{13}	0.436
2.38	1.435_5	0.568	1.902_3	0.516	1.889_5	0.525	1.800_6	0.519	2.018_{13}	0.444
2.48	1.365_2	0.586	1.714_3	0.535	1.754_4	0.543	1.677_7	0.537	2.096_{12}	0.460
2.53	1.357_1	0.594	1.682_3	0.544	1.680_5	0.552	1.599_7	0.546	2.296_{12}	0.468
2.64	1.263_1	0.611	1.461_4	0.562	1.512_7	0.570	1.555_7	0.564	2.416_{12}	0.484
2.69	1.262_6	0.620	1.438_3	0.571	1.517_8	0.579	1.311_8	0.573	2.366_{13}	0.492
2.80	1.118_9	0.636	1.378_6	0.588	1.372_3	0.596	1.241_8	0.591	2.333_{13}	0.508
2.86	1.119_7	0.644	1.284_3	0.597	1.379_5	0.605	1.212_8	0.599	1.973_{13}	0.516
2.98	1.126_4	0.659	1.294_2	0.614	1.284_6	0.622	1.156_8	0.616	1.540_{14}	0.531
3.04	1.074_3	0.667	1.302_3	0.622	1.215_7	0.630	1.165_8	0.624	1.572_{14}	0.539
3.17	0.945_7	0.680	1.286_5	0.638	1.268_5	0.645	1.148_8	0.640	1.625_{14}	0.553
3.23	1.004_1	0.687	1.259_5	0.645	1.336_9	0.653	1.032_{11}	0.647	1.668_{18}	0.561
3.36	0.989_1	0.700	1.288_4	0.660	1.273_8	0.668	0.993_{11}	0.663	1.913_{17}	0.575
3.43	1.015_3	0.706	1.225_7	0.668	1.220_8	0.675	0.986_{11}	0.670	1.929_{17}	0.582
3.57	1.033_2	0.718	1.345_8	0.682	1.259_{11}	0.689	1.070_{10}	0.684	1.441_{19}	0.596
3.65	0.989_1	0.724	1.216_5	0.689	1.214_{10}	0.696	0.988_{10}	0.691	1.350_{19}	0.603
3.80	0.962_1	0.735	1.255_5	0.703	1.188_8	0.710	0.938_{11}	0.705	1.565_{18}	0.616
3.88	0.959_6	0.741	1.241_6	0.710	1.087_{10}	0.716	0.938_{11}	0.712	1.558_{18}	0.623
3.95	0.932_1	0.746	1.160_8	0.716	1.197_7	0.722	1.020_{10}	0.718	1.703_{17}	0.630
4.04	0.942_1	0.751	1.163_3	0.722	1.126_9	0.728	0.903_{11}	0.724	1.558_{18}	0.636
4.12	0.994_4	0.756	1.139_7	0.728	1.131_8	0.734	0.848_{12}	0.730	1.440_{19}	0.642
4.29	0.905_8	0.764	1.038_6	0.739	1.082_9	0.745	0.780_{13}	0.741	1.493_{18}	0.653
4.38	0.868_1	0.768	1.056_7	0.745	1.038_8	0.750	0.777_{13}	0.746	1.398_{19}	0.659
4.56	0.857_3	0.777	0.980_6	0.755	1.001_9	0.760	0.732_{13}	0.757	1.375_{19}	0.671
4.65	0.841_1	0.781	0.960_5	0.760	0.934_{10}	0.765	0.628_{16}	0.762	1.224_{21}	0.676
4.84	0.719_5	0.789	0.885_6	0.770	0.889_7	0.775	0.653_{16}	0.771	1.345_{20}	0.687
4.94	0.752_4	0.793	0.892_5	0.775	0.900_{10}	0.780	0.641_{16}	0.776	1.278_{20}	0.692
5.14	0.710_9	0.800	0.877_4	0.784	0.908_{11}	0.788	0.664_{15}	0.785	1.233_{21}	0.702
5.25	0.667_9	0.803	0.889_8	0.788	0.858_{12}	0.792	0.608_{17}	0.789	1.080_{23}	0.707
5.47	0.696_4	0.810	0.880_8	0.796	0.825_{14}	0.800	0.595_{18}	0.797	1.092_{23}	0.717
5.58	0.696_2	0.813	0.851_5	0.800	0.856_{13}	0.803	0.536_{20}	0.801	1.034_{24}	0.721
5.81	0.649_1	0.820	0.809_6	0.807	0.845_8	0.811	0.514_{22}	0.808	1.050_{24}	0.731

Table A3. (Contiuned.)

x	Fat		Muscle		Liver		Kidney		Bone	
(nm^{-1})	F_{coh}	F_{inc}	F_{coh}	F_{inc}	F_{coh}	F_{inc}	F_{coh}	F_{inc}	F_{coh}	F_{inc}
5.93	0.670_{1}	0.823	0.814_{9}	0.811	0.780_{14}	0.814	0.504_{23}	0.812	1.035_{24}	0.735
6.17	0.605_{12}	0.830	0.683_{10}	0.818	0.643_{9}	0.821	0.607_{17}	0.819	1.087_{18}	0.744
6.30	0.591_{9}	0.833	0.766_{9}	0.821	0.717_{6}	0.824	0.502_{22}	0.822	1.049_{19}	0.748
6.56	0.568_{10}	0.839	0.710_{12}	0.827	0.654_{13}	0.831	0.414_{31}	0.828	1.054_{24}	0.757
6.69	0.614_{6}	0.842	0.703_{9}	0.830	0.656_{12}	0.834	0.315_{50}	0.831	0.972_{25}	0.761
6.97	0.662_{11}	0.849	0.724_{11}	0.837	0.660_{16}	0.840	0.353_{43}	0.838	0.970_{26}	0.769
7.11	0.549_{16}	0.852	0.723_{12}	0.840	0.650_{15}	0.843	0.468_{25}	0.841	1.016_{20}	0.774
7.40	0.582_{1}	0.859	0.679_{14}	0.846	0.591_{10}	0.849	0.508_{22}	0.847	0.958_{21}	0.782
7.87	0.520_{3}	0.869	0.757_{9}	0.855	0.659_{5}	0.858	0.460_{29}	0.856	0.839_{30}	0.794
8.03	0.586_{3}	0.872	0.743_{15}	0.858	0.616_{18}	0.861	0.431_{32}	0.859	0.923_{27}	0.798
8.70	0.535_{2}	0.885	0.715_{13}	0.869	0.640_{15}	0.873	0.328_{51}	0.870	0.757_{34}	0.815
9.25	0.534_{13}	0.895	0.638_{16}	0.878	0.484_{16}	0.882	0.369_{42}	0.879	0.762_{34}	0.827

References

Berger M J, Hubbell J H, Seltzer S M, Chang J, Coursey J S, Sukumar R, Zucker D S and Olsen K 2010 *XCOM: Photon Cross Section Database* version 1.5 (Gaitherbsurg, MD: National Institute of Standards and Technology) http://physics.nist.gov/xcom

Castro C R F, Barroso R C, Anjos M J, Lopes R T and Braz D 2004 Coherent scattering characteristics of normal and pathological breast human tissues *Radiat. Phys. Chem.* **71** 649–51

Desouky O S, Elshemey W M, Selim N S and Ashour A H 2001 Analysis of low-angle x-ray scattering peaks from lyophilized biological samples *Phys. Med. Biol.* **46** 2099–106

Elshemey W M, Desouky O S, Fekry M M, Talaat S M and Elsayed A A 2010 The diagnostic capability of x-ray scattering parameters for the characterization of breast cancer *Med. Phys.* **37** 4257–65

Evans S H, Bradley D A, Dance D R, Bateman J E and Jones C H 1991 Measurement of small-angle photon scattering for some breast tissues and tissue substitute materials *Phys. Med. Biol.* **36** 7–18

Fernández M, Keyriläinen J, Serimaa R, Torkkeli M, Karjalainen-Lindsberg M-L, Tenhunen M, Thomlinson W, Urban V and Suortti P 2002 Small-angle x-ray scattering studies of human breast tissue samples *Phys. Med. Biol.* **47** 577–92

Griffiths J A, Royle G J, Hanby A M, Horrocks J A, Bohndiek S E and Speller R D 2007 Correlation of energy dispersive diffraction signatures and microCT of small breast tissue samples with pathological analysis *Phys. Med. Biol.* **52** 6151–64

Hasan M Z 2003 Measurement of x-ray scattering form factors over a wide momentum transfer range *MSc Thesis* Department of Physics, Carleton University, Ottawa, Ontario, Canada

Hasan M Z and Johns P C 2004 Energy-dispersive technique to measure x-ray scattering form factors over a wide momentum transfer range *Phys. Canada* **60** 145

Hubbell J H and Øverbø I 1979 Relativistic atomic form factors and photon coherent scattering cross sections *J. Phys. Chem. Ref. Data* **8** 69–105

ICRP (International Commission on Radiological Protection) 1975 Report of the Task Group on Reference Man *ICRP Report 23* (Oxford: Pergamon)

Johns H E and Cunningham J R 1983 *The Physics of Radiology* 4th edn (Springfield, IL: Charles C Thomas)

Johns P C and Wismayer M P 2004 Measurement of coherent x-ray scatter form factors for amorphous materials using diffractometers *Phys. Med. Biol.* **49** 5233–50

Kidane G, Speller R D, Royle G J and Hanby A M 1999 X-ray scatter signatures for normal and neoplastic breast tissues *Phys. Med. Biol.* **44** 1791–802

King B W 2009 Accurate measurement of the x-ray coherent scattering form factors of tissues *PhD Thesis* Department of Physics, Carleton University, Ottawa, Ontario, Canada

King B W and Johns P C 2008 Measurement of coherent scattering form factors using an image plate *Phys. Med. Biol.* **53** 5977–90 (corrigendum **54** 6437)

King B W and Johns P C 2010 An energy-dispersive technique to measure x-ray coherent scattering form factors of amorphous materials *Phys. Med. Biol.* **55** 855–71

Kosanetzky J, Knoerr B, Harding G and Neitzel U 1987 X-ray diffraction measurements of some plastic materials and body tissues *Med. Phys.* **14** 526–32

Leclair R J, Boileau M M and Wang Y 2006 A semianalytic model to extract differential linear scattering coefficients of breast tissue from energy dispersive x-ray diffraction measurements *Med. Phys.* **33** 959–67

Leclair R J and Johns P C 2001 X-ray forward-scatter imaging: experimental validation of model *Med. Phys.* **28** 210–9

Leclair R J and Johns P C 2002 Optimum momentum transfer arguments for x-ray forward scatter imaging *Med. Phys.* **29** 2881–90

Lehmann L A, Alvarez R E, Macovski A, Brody W R, Pelc N J, Riederer S J and Hall A L 1981 Generalized image combinations in dual kVp digital radiography *Med. Phys.* **8** 659–67

Lewis R A *et al* 2000 Breast cancer diagnosis using scattered x-rays *J. Synchrotron Radiat.* **7** 348–52

Narten A H 1970 X-ray diffraction data on liquid water in the temperature range 4 °C–200 °C *Technical Report ORNL 4578* (Oak Ridge, TN: Oak Ridge National Laboratory)

Peplow D E and Verghese K 1998 Measured molecular coherent scattering form factors of animal tissues, plastics and human breast tissue *Phys. Med. Biol.* **43** 2431–52

Plechaty E F, Cullen D E and Howerton R J 1975 Tables and graphs of photon interaction cross sections from 1.0 keV to 100 MeV derived from the LLL evaluated nuclear data library *Technical Report UCRL-50400* vol 6 revision 1 (Livermore, CA: Lawrence Livermore Laboratory)

Poletti M E, Gonçalves O D and Mazzaro I 2002 X-ray scattering from human breast tissues and breast-equivalent materials *Phys. Med. Biol.* **47** 47–63

Royle G J and Speller R D 1995 Quantitative x-ray diffraction analysis of bone and marrow volumes in excised femoral head samples *Phys. Med. Biol.* **40** 1487–98

Tartari A, Casnati E, Bonifazzi C and Baraldi C 1997 Molecular differential cross sections for x-ray coherent scattering in fat and polymethyl methacrylate *Phys. Med. Biol.* **42** 2551–60

Westmore M S, Fenster A and Cunningham I A 1996 Angular-dependent coherent scatter measured with a diagnostic x-ray image intensifier-based imaging system *Med. Phys.* **23** 723–33

Woodard H Q 1962 The elementary composition of human cortical bone *Health Phys.* **8** 513–7